Bovine serum albumin promotes reactivation of viable but non-culturable *Mycobacterium tuberculosis* via the activation of protein kinase-dependent cell division processes

Yuta Morishige[1*], Yoshiro Murase[1], Kinuyo Chikamatsu[1], Hiroyuki Yamada[1], Akio Aono[1], Yuriko Igarashi[1], Keisuke Kamada[1], Yoshiko Shimomura[1], Makiko Hosoya[1], Akiko Takaki[1], and Satoshi Mitarai[1,2]

[1]Department of Mycobacterial Reference and Research, The Research Institute of Tuberculosis, Japan Anti-Tuberculosis Association, Kiyose, Tokyo, Japan.

[2]Department of Basic Mycobacteriology, Graduate School of Biomedical Sciences, Nagasaki University, Nagasaki, Japan.

*** Correspondence:**

Yuta Morishige

ymorishige@jata.or.jp

Keywords: VBNC, Mycobacterium, Albumin, Reactivation, Dormancy

Abstract

Objective: *Mycobacterium tuberculosis* (Mtb) H37Ra strain has been reported to rapidly enter the viable but non-culturable (VBNC) state following treatment with an NADH oxidase inhibitor (diphenyleneiodonium [DPI]) and to be reactivated by fetal bovine serum (FBS). However, the mechanism underlying FBS-induced reactivation is unclear. We tried to reveal the mechanism of FBS-induced reactivation using *M. tuberculosis* H37Rv.

Methods: First, we evaluated the effect of DPI on culturability, viability and changes of acid-fastness toward H37Rv. Secondly, we measured the reactivation-promoting effects of human serum albumin, egg-white albumin and antioxidative agents in DPI-induced VBNC cells. We also inhibited adenylyl cyclase and protein kinase which is the downstream of adenylyl cyclase to evaluate the influence to reactivation capacity of bovine serum albumin (BSA).

Results: DPI treatment induced VBNC state in H37Rv, resulting in a high proportion of viable cells but a low proportion of culturable cells, loss of acid-fastness and lipid-accumulation. Not only FBS but also BSA alone could reactivate H37Rv. Contrary to our expectation, only human serum albumin had a similar restorative effect to BSA. The inhibition of adenylyl cyclase by SQ22536 did not have a significant effect on reactivation; however, the inhibition of mycobacterial protein kinase by H89 and staurosporine strongly suppressed the BSA-induced reactivation.

Conclusion: DPI-induced VBNC Mtb cells may be reactivated via the activation of protein kinase-dependent cell division processes through interaction with BSA.

Introduction

Mycobacterium tuberculosis (Mtb) is known to as one of the intracellular parasitic bacteria that can survive inside host macrophages. It develops a latent phenotype, dormancy, due to various stresses such as host immune response, oxygen depletion, nutritional starvation, *etc.*

The dormant Mtb cells can persist inside the host and cause latent tuberculosis infection (LTBI), which seeks reactivation. Lowering the risk of Mtb reactivation in LTBI patients is considered to be one of the important strategies to reduce the incidence of TB (1). The dormancy phenomenon in non-sporulating bacteria has been described as two major states: the viable but non-culturable (VBNC) state and bacterial persistence (2). VBNC cells are a nonculturable population that can be induced by exposure to stress. In addition, they cannot be grown on nutrient media, even after removal of stress, and require a much longer time or specific stimulus for reactivation (2, 3). On the other hand, persistent cells are stochastically arising cells within growing cultures that are tolerant to stress, including high-dose antibiotics, and they are also growth-arrested. However, they are typically able to grow on nutrient media within a short period after the removal of stress (2).

Many pathogenic bacteria, including Mtb, can enter into the VBNC state, and it is considered to be their natural state in the environment including human body (4). Various *in vitro* models, such as models of hypoxia, nutritional starvation (including potassium-deficiency), a lipid-rich environment, and other multiple stresses are reported to induce a VBNC state in Mtb cells (5–9). A deep understanding of the mechanisms of reactivation is necessary for the prevention of active tuberculosis.

One of the major hypotheses regarding the mechanism underlying the formation of VBNC bacteria involves oxidative damage generated by harsh external conditions (10). Thus, some studies have reported that the antioxidation during culture is one of the key mechanisms through which VBNC bacteria are reactivated (11, 12). Some mycobacterial culture media contain bovine serum albumin (BSA) and BSA on mycobacterial culture has been considered to be growth-supporting agent that is involved in detoxification by the absorption of free fatty acid and other growth-suppressing agents that are spontaneously generated during culturing (13–15). For this reason, the mycobacterial culture media that are most frequently used at the present time are BSA-containing systems, such as Middlebrook 7H series or Dubos medium.

63 However, few studies have focused on the effect of such media on VBNC cells.

64 Mukamolova *et al*. revealed that among patients with active TB, there is certain
65 subpopulation for whom sputum is not culturable in conventional medium, but which becomes
66 to be culturable in the presence of resuscitation promoting factor (Rpf), which is a
67 peptidoglycan-hydrolyzing protein that is highly conserved in actinobacteria (16). Rpf
68 reactivates non-culturable Mtb cells both *in vitro* and *in vivo* (17), suggesting the presence of
69 VBNC Mtb cells in clinical specimens.

70 Previously, NADH oxidase inhibitor diphenyleneiodonium chloride (DPI) was reported to
71 simply and rapidly induce a VBNC state in the Mtb H37Ra strain, and incubation with fetal
72 bovine serum, which is a common supplement for mammalian cell cultures, could facilitate the
73 reactivation of VBNC cells, while incubation with OADC (oleate-albumin-dextrose-catalase)
74 supplementation could not (18). This report gave us an important clue for constructing a simple
75 and rapid assay system to induce and reactivate VBNC Mtb cells. However, when we tried to
76 apply this system to H37Rv, we happened to find that DPI-induced VBNC cells that could be
77 reactivated by not only fetal bovine serum but also by the addition of BSA—this was observed
78 for both H37Rv and H37Ra (internal data). Then, we hypothesized that BSA would act as a
79 reactivation-promoting agent toward DPI-induced VBNC cells.

80 One possible mechanism that may promote reactivation of BSA is its antioxidative property,
81 which has been well-studied (19). Another possibility is a cellular processes involving cyclic
82 AMP, an important second messenger of the cell. Shleeva *et al*. showed that the presence of
83 high amounts of cAMP provided by adenylyl cyclase is also essential for the reactivation of *M.*
84 *smegmatis* and Mtb from the VBNC state (20, 21). Notably, the overexpression of the Rv2212
85 gene, which encodes adenylyl cyclase in Mtb (22), significantly affects both entry into and
86 reactivation from the VBNC state (21).

87 An understanding of the detailed mechanism of reactivation from the VBNC state is crucial
88 for reducing the risk of reactivation of Mtb cells in LTBI patients. In this study, we examined

89 the effects of antioxidative agents and the inhibition of adenylyl cyclase to reveal the roles of
90 these factors in the reactivation of VBNC Mtb cells.

91 Materials and Methods

92 Bacterial strains, growth media and culture conditions

93 This work was carried out using *Mycobacterium tuberculosis* H37Rv (ATCC 27294) and
94 H37Ra (ATCC 25177). Both cells were cultured for 3–5 days in a 60 mL glycol-modified
95 polyethylene terephthalate (PETG) bottle containing 20 mL Dubos broth (2.5 g/L Na_2HPO_4,
96 2.0 g/L L-asparagine, 1.0 g/L KH_2PO_4, 0.5 g/L pancreatic digest of casein, 0.2 g/L Tween 80,
97 0.5 mg/mL $CaCl_2$•$2H_2O$, 0.1 mg/mL $CuSO_4$, 0.1 mg/mL $ZnSO_4$•$7H_2O$, 0.05 g/L ferric
98 ammonium citrate, 0.01g $MgSO_4$•$7H_2O$) with 5% (v/v) glycerol, and 10% (v/v) ADC
99 supplementation (5.0 g bovine serum albumin fraction V (BSA), 2.0 g dextrose, 0.003 g
100 catalase in 100 mL distilled water) at 37˚C in an orbital shaker (100 rpm) until the OD_{600}
101 reached up to 0.35. All procedures were performed at a BSL-3 facility. For further analysis, we
102 used commercially available BSA Cohn fraction V (Merck, Darmstadt, Germany), unless
103 otherwise stated. In addition, we used molecular biology grade Tween 80 (Merck product
104 number P5188-100ML) without any predilution.

105 Counting the number of culturable cells

106 The cultured bacterial suspension was serially diluted 10-fold in phosphate buffered saline (pH
107 6.8) with 0.1%(w/v) Tween 80 (PBS-T) and 25 μL of each diluent was inoculated onto a
108 Middlebrook 7H10 agar plate supplemented with oleic-albumin-dextrose-catalase (OADC)
109 (Becton Dickinson, Sparks, MD) in duplication. Colonies were counted after at least 3 weeks'
110 incubation at 37˚C under 5% CO_2. The limit of detection was determined to be 20 CFU/mL
111 because of the diluent factor.

112 Effect of BSA on the growth of Mtb cells in Dubos medium

113 Ten milliliters of log phase culture of Mtb H37Rv that reached an OD_{600} of up to 0.35 in Dubos
114 medium, as described previously, was sedimented at 3,000 ×*g* for 10 minutes at 4˚C and the
115 supernatant was discarded. The sediment was washed twice with fresh Dubos broth and
116 resuspended with 10 mL of Dubos broth. The suspension was diluted to 1:10 with Dubos broth
117 with or without the addition of BSA solution (5.0 g BSA fraction V in 100 mL distilled water)
118 at the final concentration of 0.1% (w/v) BSA. The diluted suspension was dispensed into 24-
119 well plates (Sarstedt, Nümbrecht, Germany) in 1.5 mL increments and sealed with gas-
120 permeable film (Breathe-Easy, Diversified Biotech Inc, Dedham, MA, United States). Cultures
121 were incubated for 5, 10, 15 and 20 days at 37˚C under 5% CO_2. At each time-point, the number
122 of culturable cells was measured as described above.

123 **Induction of the VBNC cells**

124 Induction of the VBNC cells were performed according to the previous report (18) with some
125 modification. In short, the log phase culture of Mtb H37Rv or H37Ra that reached an OD_{600} of
126 up to 0.35 in Dubos medium, as previously described, was evenly divided into 30 mL PETG
127 bottles and 5 mg/mL diphenyleneiodonium chloride (DPI) in dimethyl sulfoxide (DMSO)
128 solution was directly added at the final concentration of 4 μg/mL with immediate agitation.
129 The same volume of DMSO was added to the untreated control sample. Cultures were further
130 incubated for 24 h at 37˚C without shaking. After incubation, their culturability and viability
131 were measured as described above.

132 **Cell viability assay**

133 Mtb cell viability was measured using esterase activity and membrane integrity of the cells
134 using dual staining with 10 mg/mL carboxyfluorescein diacetate (CFDA, Dojindo, Kumamoto,
135 Japan) and ethidium bromide (EtBr, Dojindo, Kumamoto, Japan). Briefly, 500 μL of DPI-
136 treated or untreated Mtb culture was sedimented by centrifugation at 15,000 ×*g* for 5 minutes
137 at 4˚C and washed twice with the same volume of PBS-T. The washed bacterial sediment was

138 resuspended in 200 µL of PBS-T with CFDA and EtBr incubated at room temperature (RT) for
139 30 minutes in shade. The final concentration of CFDA and EtBr were 60 µg/mL and 2 µg/mL,
140 respectively. The stained Mtb cells were washed twice with PBS-T and fixed with 3.7%
141 formaldehyde solution at RT for at least 2 h. After fixation, 10 µL of bacterial suspension was
142 smeared on three APS-coated 8-well slides (Matsunami glass, Osaka, Japan) and air-dried.
143 Then the slides were mounted with DPX new non aqueous mounting medium (Merck,
144 Darmstadt, Germany) and a 150 µm-thick cover glass (Matsunami glass, Osaka, Japan) prior
145 to the microscopic observation. Specimens were examined with a BX53 fluorescence
146 microscope (Olympus, Tokyo, Japan) at a magnification of 100× for green (esterase-active with
147 intact membrane; live) or red (esterase-negative with damaged membrane; dead) fluorescing
148 cells. The excitation source for CFDA and EtBr was generated from a mercury-arc lamp (blue
149 beam, 470–495 nm; green beam, 530–550nm) using a corresponding band-pass filter. The
150 green-fluorescence emission from the CFDA-positive cells was collected through a 510–550
151 nm band-pass filter. The red-fluorescence emission from EtBr-positive cells was collected
152 through a 575 nm long-pass filter. At least 10 random fields were observed for each sample and
153 the images (TIFF format) were analyzed using the Fiji/ImageJ software program (23). The
154 live/dead ratio was calculated by direct counting of green or red fluorescing cells.

155 **Auramine-O/Nile Red dual staining**

156 Loss of acid-fastness and accumulation of neutral lipids are distinctive features of VBNC
157 mycobacteria (24). To detect the phenotype, fluorescent acid-fast staining with auramine-O and
158 neutral lipid staining with Nile Red (9-dimethylamino-5H-benzo-α-phenoxadine-5-one) were
159 performed using a previously described method (9) with some modification. Briefly, 10 µL of
160 DPI-treated or untreated culture were smeared onto an APS-coated slide (Matsunami glass,
161 Osaka, Japan) and air-dried. Then, the slide was heat-fixed and cooled down to room
162 temperature before staining. The smear was flooded with fluorochrome staining solution (10

163 μg/mL auramine-O in 5% [w/v] phenol solution) and incubated at room temperature for 20 min
164 in shade. Excessive dye was removed using 3% hydrochloric acid ethanol for 15 minutes. Next,
165 the smear was covered with 10 μg/mL Nile Red in ethanol and incubated at room temperature
166 for 15 minutes. Finally, the smear was counterstained with 0.1% (w/v) potassium permanganate
167 solution with 1 minute. Stained slides were air-dried and mounted as described previously.
168 Fluorescence microscopy was performed at 100× magnification for green (acid-fastness
169 positive, lipid accumulation negative; active) or red (acid-fastness negative, lipid accumulation
170 positive; VBNC) fluorescing cells. The excitation source for auramine-O and Nile Red was
171 generated from a mercury-arc lamp (blue beam, 470–495 nm; green beam, 530–550 nm) using
172 a corresponding band-pass filter. The green-fluorescence emission from auramine-O-positive
173 cells was collected through a 510–550 nm band-pass filter. The red-fluorescence emission from
174 Nile Red-positive cells was collected through 575 nm long-pass filter. At least 5 random fields
175 were observed for each sample and images (TIFF format) were analyzed by the Fiji/ImageJ
176 software program (23) and the proportion of acid-fast-positive cells and lipid-accumulation-
177 positive cells was calculated by direct counting of green or red fluorescing cells.

178 **Ziehl-Neelsen staining**

179 Ziehl-Neelsen staining was also performed to confirm the loss of acid-fastness resulting in the
180 VBNC state by DPI treatment, according to the standard method (25). The slide was observed
181 by light microscope under 100× magnification with an oil immersion lens (BX53, Olympus,
182 Tokyo, Japan).

183 **Confocal super-resolution microscopy**

184 Detailed images of accumulated lipids were also obtained by a confocal laser-scanning
185 microscope (LSM900 with Airyscan 2, Carl Zeiss Microscopy, Jena, Germany). Briefly, culture
186 slides of DPI-treated cells dual stained with auramine-O and Nile Red, as described above,
187 were observed at 63x magnification with oil immersion lens. The excitation source of

188 auramine-O and Nile Red was 488 nm (blue beam) and 563 nm (green beam), from a solid-
189 state laser unit. The green-fluorescence emission from auramine-O and red fluorescence from
190 Nile Red were sequentially collected through a variable dichroic beamsplitter and an Airyscan
191 2 detector. Super-resolution images were processed with the ZEN Blue software program (Carl
192 Zeiss, Jena, Germany).

193 **VBNC reactivation assay**

194 The VBNC reactivation assay was performed as described elsewhere (18) with some
195 modification. DPI-treated culture was sedimented by centrifugation at 3,000 x*g* for 10 minutes
196 at 4˚C and washed twice with fresh Dubos broth, then resuspended in ten-milliliters of Dubos
197 broth. The bacterial suspension was diluted to 1:10 with fresh Dubos medium with or without
198 0.1% (w/v) BSA. For both BSA-containing and BSA-free series, OADC supplementation
199 (Becton Dickinson, Sparks, MD), fetal bovine serum (FBS; Moregate BioTech, Bulimba,
200 Queensland, Australia), or sodium pyruvate (PA; Merck) was added. The final concentration
201 of each reagent was as follows: 10% (v/v) for OADC supplementation, 2% (v/v) for FBS, and
202 3 mM for PA. Then, the diluted suspension was dispensed into 24-well plates in 1.5 mL
203 increments and sealed with gas-permeable film. Cultures were incubated for 5, 10, 15 and 20
204 days at 37˚C under 5% CO_2. At each time-point, the number of culturable cells was measured
205 as described previously.

206 **Evaluation of the reactivation-promoting effect of human serum albumin, egg-white**
207 **albumin (ovalbumin) and antioxidative agents**

208 To determine whether the reactivation-promoting effect of BSA is its antioxidative property,
209 we measured the reactivation-promoting activity of other albumins and antioxidative agents
210 toward DPI-treated Mtb cells. Washed DPI-treated cells were resuspended with fresh Dubos
211 broth without BSA and the suspension was diluted to 1:10 with Dubos broth containing BSA,
212 human serum albumin (HSA), ovalbumin (OVA), N-acetyl-*L*-cysteine (NAC) or D-mannitol

213 (MAN). The final concentration of each reagent was 0.1% (w/v) for BSA, HSA and OVA, 500
214 μM for NAC, and 50 mM for MAN, respectively. Then, the diluted suspension was dispensed
215 into 24-well plates in 1.5 mL increments and sealed with gas-permeable film. The plate was
216 incubated for 20 days at 37˚C under 5% CO_2. At the end of incubation, the number of colonies
217 grown was measured as described previously.

218 **Evaluation of the reactivation-promoting effect of fatty acid and globulin-free BSA**

219 To determine the effect of BSA Cohn fraction V contaminants, we measured the reactivation-
220 promoting activity of fatty acid and globulin-free BSA toward DPI-treated VBNC Mtb cells.
221 Washed DPI-treated cells were resuspended with fresh Dubos broth without BSA and the
222 suspension was diluted to 1:10 with Dubos broth containing BSA Cohn fraction V or fatty acid
223 and globulin-free BSA. Fatty acid and globulin-free BSA were acquired from Merck. The final
224 concentration of both BSAs was 0.1% (w/v). The number of culturable cells was measured as
225 described previously.

226 **Effects of adenylyl cyclase or protein kinase on BSA-induced reactivation**

227 Washed DPI-treated VBNC Mtb cells were resuspended with fresh Dubos broth and the
228 suspension was diluted to 1:10 with Dubos broth with 0.1% (w/v) BSA containing adenylyl
229 cyclase inhibitor SQ22536 (Merck, Darmstadt, Germany) or protein kinase inhibitor H89
230 (Abcam, Cambridge, United Kingdom) or staurosporine (Merck). The final concentration of
231 each inhibitor was as follows: 0.1 to 10 mM for SQ22536, 1 to 30 μM for H89 and 1 to10 μM
232 for staurosporine. Then, the number of culturable cells were measured as described previously.

233 **Molecular docking simulation**

234 A molecular docking simulation was performed using the AutoDock Vina software program,
235 an open-source molecular docking program designed by the Scripps Research Institute (26, 27).
236 The 3D structures of receptor proteins, PknA and Rv2212, were obtained from the Protein Data

237 Bank (28) and AlphaFold Database (29, 30), respectively. The PDB ID for PknA was 4OW8
238 (31) and the AlphaFold Database identifier for Rv2212 was AF-P9WMU7-F1. We removed
239 water molecules from proteins, added polar hydrogen and charge, and adjusted the X-Y-Z
240 coordinates and grid size to optimize molecular docking. The 3D structures of ligand molecules,
241 H89, SQ22536 and ATP were obtained from the PubChem Database. The PubChem CIDs of
242 each ligand were 449241, 5270 and 5957, respectively. Graphical processing was performed
243 using the Chimera software program (32).

244 **Statistical analysis**

245 The statistical analysis was performed with R (33) using the EZR on R package (34). *P* values
246 of < 0.05 were considered statistically significant.

247 **Results**

248 **I. BSA is not essential for the growth of MTB in Dubos medium with purified non-**
249 **prediluted Tween 80**

250 Figure 1 shows the different effects of BSA-containing and BSA-free Dubos medium on the
251 growth of Mtb H37Rv. As shown in Fig. 1(A), the growth rates with the two conditions did not
252 differ to a statistically significant extent. Fig. 1(B) also shows the sufficient growth of cells.
253 The cells were more aggregative without BSA; however, the aggregation was easily dispersed
254 by pipetting and there was no significant difference in the OD_{600} value. The albumin component
255 was inessential for Mtb growth.

256 **II. DPI treatment induced a VBNC state in Mtb H37Rv**

257 Figure 2 shows the DPI treatment results for the induction of VBNC state in H37Rv and
258 H37Ra (18). As shown in Fig. 2(A), the numbers of culturable cells of untreated control

259 population and DPI-treated population were significantly different: $4.43 \pm 1.43 \times 10^8$ CFU/mL
260 for the untreated control population and $4.64 \pm 6.10 \times 10^3$ CFU/mL for DPI-treated population.
261 Fig. 2(B) shows that the CFDA-positive cells in the untreated control and DPI-treated
262 populations were 81.8 ± 11.4% and 65.9 ± 11.8%, respectively. These results suggested that
263 the majority of DPI-treated H37Rv cells were alive ($p = 0.169$), while their culturability was
264 significantly reduced ($p = 0.033$). Representative images of CFDA/EtBr dual-stained cells of
265 the untreated control and DPI-treated population also showed that there was little difference in
266 the proportions of CFDA-positive and EtBr-positive cells. (Fig. 2[C])

267 Auramine-O/Nile Red dual staining showed the reduction of acid-fastness and the
268 accumulation of the neutral lipid. As shown in Fig. 2(D), the proportion of acid-fast-
269 negative/lipid accumulation-positive cells was 84.0 ± 14.0% in the DPI-treated population, and
270 12.1 ± 11.9% in the untreated control population ($p < 0.01$). Representative images of
271 auramine-O/Nile Red dual-stained cells of the untreated control and DPI-treated populations
272 also showed that there were distinctive differences in the proportions of acid-fast-positive cells
273 and lipid-accumulation-positive cells (Fig. 2[E]). The loss of acid-fastness was also confirmed
274 by Ziehl-Neelsen staining; the majority of DPI-treated population were found to have lost their
275 acid-fastness (Suppl. Fig. 1). Interestingly, Airyscan microscopy revealed some DPI-treated
276 cells were both acid-fast stain-positive and neutral lipid stain-positive (Fig. 2[F]). These results
277 indicated that DPI treatment induced the VBNC state in H37Rv as well as in H37Ra.

278 III. The effects of BSA, FBS, OADC and sodium pyruvate on the reactivation of DPI-
279 treated VBNC Mtb cells

280 As shown in Fig. 3(A) and (B), our results partially support the previous study (18) with
281 some differences; although the culturability of DPI-treated H37Rv cells was restored by
282 incubation with FBS-supplemented medium, OADC-supplemented medium could also induce
283 culturability. The addition of albumin alone into the medium could also induce reactivation.

284 The addition of FBS in BSA-free Dubos medium slightly reduced the regrowth rate; however,
285 cells were successfully reactivated at the end of incubation with or without FBS. These
286 phenomena were also observed in H37Ra (Suppl. Fig 2). Thus, we used the H37Rv strain for
287 the further analyses in this study.

288 Incubation with sodium pyruvate, which was reported to have a reactivation-promoting
289 effect on VBNC cells elsewhere, led to transient regrowth by day 15 and a slight reduction at
290 day 20. (Suppl. Fig. 3[A] and [B]).

291 We also confirmed the presence of a small population of intact Mtb cells (10^3 CFU/mL) that
292 could grow normally in BSA-free Dubos medium, suggesting that the reactivation might not
293 be due to the presence of a small number of culturable cells after DPI-treatment (data not
294 shown).

295 **IV. The antioxidative property or the fatty acid from BSA did not promote**
296 **reactivation.**

297 As shown in Fig. 4(A) and (B), the reactivation-promoting effect of BSA was specific to
298 bovine and human serum albumin. Ovalbumin did not show a reactivation-promoting effect
299 but maintained the number of culturable cells in this system. NAC (antioxidative agent) and
300 D-mannitol (free radical scavenger) did not show any reactivation capacity.

301 We also checked whether the purity of albumin affects the promotion of reactivation using
302 fatty acid and globulin-free BSA and confirmed that there was no significant difference in
303 reactivation-promoting effects (Suppl. Fig 4). These results suggest that commercially
304 available albumin including fatty acids do not affect the reactivation of DPI-treated Mtb.

305 **V. The reactivation-promoting effect of albumin was canceled by treatment with**
306 **eukaryotic protein kinase inhibitor.**

307 As shown in Fig. 5(A) and (B), SQ22536, adenylyl cyclase inhibitor, only suppressed
308 reactivation at a very high concentration (10 mM) in this study. However, H89, a eukaryotic
309 protein kinase inhibitor, suppressed reactivation in a dose-responsive manner. In detail,
310 incubation with 10 μM or 30 μM H89 resulted in a CFU/mL value for $3.42 \times 10^6 \pm 7.45 \times 10^5$
311 CFU/mL and $3.63 \pm 1.70 \times 10^2$ CFU/mL, while incubation without H89 resulted in 3.00×10^8
312 $\pm 5.07 \times 10^7$ CFU/mL. We also confirmed that staurosporine, which is known as mycobacterial
313 protein kinase PknB inhibitor (35), suppressed reactivation at a concentration of 10 μM and
314 resulted in a CFU/mL value of $2.09 \times 10^3 \pm 7.62 \times 10^2$ CFU/mL, while incubation without
315 staurosporine resulted in $3.58 \times 10^8 \pm 5.78 \times 10^7$ CFU/mL (Fig 5[A] and [B]). None of the
316 inhibitors used in this study caused a reduction of the growth of intact MTB cells (Suppl. Fig.
317 5A and 5B).
318 We also performed a molecular docking simulation of these inhibitors toward their
319 considerable targets on Mtb. As shown in Suppl. Table 1, both SQ22536 and H89 have
320 sufficient affinity toward Rv2212 (adenylyl cyclase) and PknA (protein kinase), respectively.

321 **Discussion**

322 In this study, we confirmed that DPI could induce a VBNC state in H37Rv as well as H37Ra.
323 The mechanism underlying the effect of DPI is considered to involve the inhibitory effect of
324 NADH oxidase, which results in the inhibition of the electron transport system of Mtb. This
325 may induce a hypoxic response in the liquid culture, resulting in a significant decrease of
326 culturability (Fig.2[A]). However, viability was highly retained (65.9%), suggesting that the
327 majority of the cells transformed to VBNC (Fig. 2[B]). Additionally, VBNC transformation
328 was confirmed by auramine-O and Nile Red staining. The loss of acid-fastness and the
329 accumulation of neutral lipids are distinctive features of VBNC mycobacterial cells.
330 Our data also demonstrated that the majority of DPI-treated Mtb H37Rv cells were stained
331 with Nile Red alone (Fig. 2[D]). Airyscan super-resolution microscopy showed the presence of

332 cells that were stained with auramine-O and which contained an intracellular lipid body stained
333 with Nile Red (Fig. 2[F]). This could also reveal the distribution of the lipid body in the cell as
334 some foci of relatively strong signals of Nile Red, suggesting the transformation from a
335 growing state to VBNC, with drastic alteration of the lipid metabolism.

336 Secondly, we found that DPI-induced VBNC could facilitate reactivation not only by
337 incubation with FBS but also with OADC supplementation and BSA alone, suggesting that
338 albumin might act as a reactivation-promoting agent in both H37Rv and H37Ra (Fig .3 and
339 Suppl. Fig. 2). These findings were contrary to the findings of the previous study, which
340 showed that only FBS can facilitate reactivation (18). We considered that the reason for the
341 difference may be due to a contaminant in Tween 80: the presence of an excessive amount of
342 oleic acid. We also confirmed that the reactivation was not facilitated by the use of prediluted
343 Tween 80 for the preparation of Dubos medium (internal data) for both H37Rv and H37Ra.
344 Thus, our results suggested that the key reactivation-promoting agent in FBS might be serum
345 albumin, and further analyses were performed using H37Rv.

346 We also tested the reactivation-promoting effect of BSA in Wayne's hypoxic culture, which
347 is widely used for inducing a VBNC of Mtb, and found that there was no significant difference
348 between cultures with and without BSA (data not shown).

349 Pyruvate, which is known to act as reactivation promoting agent for both gram-negative
350 bacteria, such as *Escherichia, Legionella, Vibrio* and gram-positive bacteria such as
351 *Staphylococcus* (36–39), did not show any reactivation-promoting effect in our experiment
352 (Suppl. Fig.3). Vilhena *et al.* reported that their proteomic analysis of VBNC *E. coli* cells
353 during reactivation revealed that enzymes involved in pyruvate metabolism, pyruvate formate-
354 lyase-activating protein (PflA), phosphoenolpyruvate carboxykinase (PckA) and lactate
355 dehydrogenase (LldD), were significantly upregulated (40), while Wagley *et al.* also reported
356 that VPA1499, an LldD homologue of Vibrio parahaemolyticus, was significantly upregulated
357 in VBNC *V. parahaemolyticus* and that depletion of LldD led to quicker entry to the VBNC

358 state (41). Interestingly, they showed that the addition of pyruvate, the product of lactate
359 oxidation, to LldD-depleted mutant restored the wild-type characteristics of cells in the VBNC
360 state. Their studies might give some crew of the lack of reactivation-promoting effect toward
361 mycobacterial VBNC. Since Mtb does not have a catalytic center of pyruvate formate-lyase
362 (PflB), pyruvate might not be able to act as reactivation-promoting agent, although pyruvate
363 enhances the growth of Mtb and *M. bovis* both intracellular and extracellular growth by
364 promoting TCA cycle and other energy-producing pathways. (42, 43).

365 Our results showed that the reactivation promoting effect of albumin might be structure-
366 specific because ovalbumin (OVA) did not facilitate reactivation, but bovine (BSA) and human
367 serum albumin (HSA) did. Focusing on their amino acid sequences, BSA and HSA share 76%
368 sequence homology (44); however, BSA and OVA share less sequence homology (16%). One
369 of the considerable roles of albumin may be as an antioxidative agent due to its cysteine
370 residues with free thiols (19, 45). BSA and HSA have only one cysteine residue with free thiol,
371 while OVA has four cysteines with free thiols (46). OVA therefore seems to be more reductive
372 than BSA and HSA. Our results were paradoxical in relation to this hypothesis; however, Davis
373 and Dubos showed the differential growth-promoting effect of albumin toward Mtb. Their
374 study supplied some interesting clues for our present study; ovalbumin does not show a growth-
375 promoting effect, while bovine and human serum albumin showed the effect (15). Moreover,
376 the antioxidative agents used in this study, NAC and D-mannitol, showed any restorative
377 effects (Fig. 4). We also examined catalase, a component of OADC supplementation, and its
378 reactivation promoting effect toward VBNC *Corynebacterium, Lactobacillus, Salmonella,*
379 *Ralstonia* and *Vibrio* (47–52); no restorative effects were observed (data not shown). These
380 results suggest that the effect of albumin may be due to complex functions rather than its
381 antioxidative property.

382 Serum albumin is known to act as a good carrier of many kinds of biologically active
383 substances, including free fatty acid. It is also known as a detoxifier of growth-arresting

384 substances in culture medium. BSA is added to mycobacterial culture medium as both a carrier
385 and detoxifier of growth-supporting and growth-arresting substances, respectively. Shleeva *et*
386 *al*. showed that several types of unsaturated free fatty acid, including oleic, linoleic, and
387 arachidonic acids, can promote the reactivation of VBNC *M. smegmatis* in modified Sauton's
388 medium and oleic acid also works for Mtb (20). In this study, we should note that impurities
389 of albumin did not affect reactivation. Although the underlying mechanism is still unclear, both
390 fatty acid and globulin-free BSA and BSA Cohn fraction V showed a similar reactivation-
391 promoting effect toward DPI-treated Mtb (Suppl. Fig. 4).

392 The reactivation inhibition assay by SQ22536, H89 and staurosporine gave us an important
393 clue for understanding the effect of BSA. In the present study, we could suppress the
394 reactivation of DPI-induced VBNC cells by inhibiting adenylyl cyclase only with a very high
395 concentration of SQ22536. Although the underlying mechanism is unclear, adenylyl cyclase
396 may not play a key role in reactivation from a DPI-induced VBNC state, while the inhibition
397 of protein kinase by H89 and staurosporine clearly suppressed reactivation. These results
398 suggest that protein kinase might mainly be involved in the reactivation of VBNC Mtb cells
399 triggered by BSA and that the contribution of adenylyl cyclase may be smaller than that of
400 protein kinase.

401 Mtb has the eukaryotic-type Ser/Thr protein kinases PknAB and PknD-L. For example,
402 PknA regulates major cell processes, regulates several types of proteins involved with
403 mycobacterial cell division and morphogenesis via phosphorylation of such proteins in
404 coordination with PknB (Manuse *et al*., 2016; Carette *et al*., 2018); phosphorylation of GlmU
405 (Rv1018c) and MurD (Rv2155c), Wag31 (Rv2145c), HupB (Rv2986c) and ParB (Rv3917c),
406 influence the production and cross-linking of peptidoglycan precursors (55–58), the spatial
407 localization of peptidoglycan synthesis (59), DNA condensation and partitioning (60, 61),
408 respectively. It should be noted that the phosphorylation of FtsZ and FipA by PknA controls
409 cell division under oxidative stress (62, 63). In addition, mycobacterial protein kinase has

410 cyclic AMP-dependent protein kinase domains which is very similar to eukaryotic version,
411 which was shown in PknB (64) and staurosporine, which act as PknB inhibitor, could also
412 inhibit reactivation of DPI-induced VBNC Mtb (Fig. 5).

413 Our study suggested that the inhibition of mycobacterial protein kinase by H89 and
414 staurosporine seems to critically affect several important cellular processes, followed by
415 reactivation (Fig. 6). To confirm the essentiality of mycobacterial protein kinase and other
416 involved proteins toward reactivation from this DPI-induced VBNC state by albumin, further
417 studies using experiments such as knock-down of genes using the CRISPR interference
418 (CRISPRi) technique (65), because such proteins—with the exception of FipA (Rv0019c)—
419 are known to be essential for *in vitro* growth (66–69); thus, manipulating their coding genes is
420 not permissible.

421 **Conclusion**

422 Our data showed that the presence of BSA in Dubos medium not only depleted growth-
423 suppressing substances but also could trigger the reactivation of the DPI-induced VBNC state
424 in both H37Rv and H37Ra strains. The reactivation-promoting effect of other kinds of
425 albumins and antioxidative agents, including NAC and D-mannitol was tested; however, only
426 human serum albumin showed a reactivation-promoting effect. The results of the inhibition
427 assay of reactivation using SQ22536, H89 and staurosporine suggests the possibility that the
428 inhibition of mycobacterial protein kinase suppressed reactivation to a much greater extent than
429 adenylyl cyclase, indicating the presence of a reactivation-promoting pathway that is protein
430 kinase-dependent.

431 To the best of our knowledge, few studies have focused on the reactivation-promoting effect
432 of albumin toward VBNC Mtb. Taken together, our findings indicated that the reactivation of
433 MTB from a DPI-induced VBNC state could be obtained by interaction with bovine serum
434 albumin and the mechanism of albumin-induced reactivation may involve the activation of

435 mycobacterial protein kinase, which regulates several important processes of cellular
436 component construction and cell division. Although it remains unclear how albumin interacts
437 with VBNC cells, our study may supply some important clues to understanding the physiology
438 of the mycobacterial VBNC state.

439 **Author Contributions**

440 YMori, YMura and SM conceived and designed the experiments. YMori performed
441 experiments. YMura, KC, AA, YI, YS, MH, KK, HY, AT, and SM assisted in the experiments.
442 YMori acquired data and YMori and YMura analyzed data. YMori performed molecular
443 docking simulation and statistical analysis. YMori and SM wrote the manuscript. All authors
444 contributed to the article and approved the submitted version.

445 **Funding**

446 This work was supported by Research Program on Emerging and Re-emerging Infectious
447 Diseases of Japan Agency for Medical Research and Development (AMED) and Grant-in-Aid
448 for Early-Career Scientists of Japan Society for the Promotion of Science (JSPS) KAKENHI.
449 Grant Numbers are JP21fk0108090 and 21K15442, respectively.

450 **Acknowledgments**

451 Authors thank Dr. K. Suenaga and Mr. H. Sakuma (Carl Zeiss Co., Ltd., Tokyo, Japan) for their
452 kind assistance in obtaining super-resolution images. Authors also thank Dr. A. Osugi (The
453 Research Institute of Tuberculosis, Japan Anti-Tuberculosis Association) for valuable
454 discussions. Authors also thank Dr. Brian Quinn (Japan Medical Communication. Inc.) for the
455 help in the preparation of this manuscript.

456 **Conflict of Interest Statement**

The authors declare that the research was conducted in the absence of any commercial or financial relationships that could be construed as a potential conflict of interest.

460 **References**

461 1. World Health Organization. 2020. TB disease burden, p. Chapter 4, 23. *In* Global
462 Tuberculosis Report 2020.
463 2. Ayrapetyan M, Williams T, Oliver JD. 2018. Relationship between the Viable but
464 Nonculturable State and Antibiotic Persister Cells. J Bacteriol 200.
465 3. Li L, Mendis N, Trigui H, Oliver JD, Faucher SP. 2014. The importance of the viable
466 but non-culturable state in human bacterial pathogens. Front Microbiol 5:258.
467 4. Oliver JD. 2010. Recent findings on the viable but nonculturable state in pathogenic
468 bacteria. FEMS Microbiol Rev 34:415–425.
469 5. Wayne LG, Hayes LG. 1996. An in vitro model for sequential study of shiftdown of
470 *Mycobacterium tuberculosis* through two stages of nonreplicating persistence. Infect
471 Immun 64:2062–2069.
472 6. Betts JC, Lukey PT, Robb LC, McAdam RA, Duncan K. 2002. Evaluation of a
473 nutrient starvation model of *Mycobacterium tuberculosis* persistence by gene and
474 protein expression profiling. Mol Microbiol 43:717–31.
475 7. Salina EG, Waddell SJ, Hoffmann N, Rosenkrands I, Butcher PD, Kaprelyants AS.
476 2014. Potassium availability triggers *Mycobacterium tuberculosis* transition to, and
477 resuscitation from, non-culturable (dormant) states. Open Biol 4.
478 8. Aguilar-Ayala DA, Cnockaert M, Vandamme P, Palomino JC, Martin A, Gonzalez-Y-
479 Merchand J. 2018. Antimicrobial activity against *Mycobacterium tuberculosis* under in
480 vitro lipid-rich dormancy conditions. J Med Microbiol 67:282–285.
481 9. Deb C, Lee CM, Dubey VS, Daniel J, Abomoelak B, Sirakova TD, Pawar S, Rogers L,
482 Kolattukudy PE. 2009. A novel in vitro multiple-stress dormancy model for
483 *Mycobacterium tuberculosis* generates a lipid-loaded, drug-tolerant, dormant pathogen.
484 PLoS One 4:e6077.

485 10. Desnues B, Cuny C, Grégori G, Dukan S, Aguilaniu H, Nyström T. 2003. Differential
486 oxidative damage and expression of stress defence regulons in culturable and non-
487 culturable *Escherichia coli* cells. EMBO Rep 4:400–404.
488 11. Imazaki I, Nakaho K. 2009. Temperature-upshift-mediated revival from the sodium-
489 pyruvate-recoverable viable but nonculturable state induced by low temperature in
490 *Ralstonia solanacearum*: linear regression analysis. J Gen Plant Pathol 2009 753
491 75:213–226.
492 12. Mizunoe Y, Wai SN, Ishikawa T, Takade A, Yoshida S. 2000. Resuscitation of viable
493 but nonculturable cells of *Vibrio parahaemolyticus* induced at low temperature under
494 starvation. FEMS Microbiol Lett 186:115–120.
495 13. Lynn M, Wilson AR, Solotorovsky M. 1979. Role of bovine serum albumin in the
496 nutrition of *Mycobacterium tuberculosis*. Appl Environ Microbiol 38:806–810.
497 14. Dubos RJ. 1947. THE EFFECT OF LIPIDS AND SERUM ALBUMIN ON
498 BACTERIAL GROWTH. J Exp Med 85:9–22.
499 15. Davis BD, Dubos RJ. 1947. THE BINDING OF FATTY ACIDS BY SERUM
500 ALBUMIN, A PROTECTIVE GROWTH FACTOR IN BACTERIOLOGICAL
501 MEDIA. J Exp Med 86:215–228.
502 16. Mukamolova G V, Murzin AG, Salina EG, Demina GR, Kell DB, Kaprelyants AS,
503 Young M. 2006. Muralytic activity of *Micrococcus luteus* Rpf and its relationship to
504 physiological activity in promoting bacterial growth and resuscitation. Mol Microbiol
505 59:84–98.
506 17. Mukamolova G V., Turapov O, Malkin J, Woltmann G, Barer MR. 2010.
507 Resuscitation-promoting factors reveal an occult population of tubercle bacilli in
508 sputum. Am J Respir Crit Care Med 181:174–180.
509 18. Yeware A, Gample S, Agrawal S, Sarkar D. 2019. Using diphenyleneiodonium to
510 induce a viable but non-culturable phenotype in *Mycobacterium tuberculosis* and its

511 metabolomics analysis. PLoS One 14:e0220628.

512 19. Roche M, Rondeau P, Singh NR, Tarnus E, Bourdon E. 2008. The antioxidant
513 properties of serum albumin. FEBS Lett 582:1783–1787.

514 20. Shleeva M, Goncharenko A, Kudykina Y, Young D, Young M, Kaprelyants A. 2013.
515 Cyclic amp-dependent resuscitation of dormant mycobacteria by exogenous free fatty
516 acids. PLoS One 8:e82914.

517 21. Shleeva MO, Kondratieva TK, Demina GR, Rubakova EI, Goncharenko A V., Apt
518 AS, Kaprelyants AS. 2017. OVerexpression Of adenylyl cyclase encoded by the
519 *Mycobacterium tuberculosis* Rv2212 gene confers improved fitness, accelerated
520 recovery from dormancy and enhanced virulence in mice. Front Cell Infect Microbiol
521 7:370.

522 22. Knapp GS, Lyubetskaya A, Peterson MW, Gomes ALC, Ma Z, Galagan JE,
523 McDonough KA. 2015. Role of intragenic binding of cAMP responsive protein (CRP)
524 in regulation of the succinate dehydrogenase genes Rv0249c-Rv0247c in TB complex
525 mycobacteria. Nucleic Acids Res 43:5377–93.

526 23. Schindelin J, Arganda-Carreras I, Frise E, Kaynig V, Longair M, Pietzsch T, Preibisch
527 S, Rueden C, Saalfeld S, Schmid B, Tinevez J-Y, White DJ, Hartenstein V, Eliceiri K,
528 Tomancak P, Cardona A. 2012. Fiji: an open-source platform for biological-image
529 analysis. Nat Methods 2012 97 9:676–682.

530 24. Garton NJ, Christensen H, Minnikin DE, Adegbola RA, Barer MR. 2002. Intracellular
531 lipophilic inclusions of mycobacteria in vitro and in sputum. Microbiology 148:2951–
532 2958.

533 25. Weyer K. 1998. Laboratory services in tuberculosis control.Part II. WHO Tech Bull
534 98:258.

535 26. Trott O, Olson AJ. 2010. AutoDock Vina: improving the speed and accuracy of
536 docking with a new scoring function, efficient optimization, and multithreading. J

537 Comput Chem 31:455–61.

538 27. Eberhardt J, Santos-Martins D, Tillack AF, Forli S. 2021. AutoDock Vina 1.2.0: New
539 Docking Methods, Expanded Force Field, and Python Bindings. J Chem Inf Model
540 61:3891–3898.

541 28. Berman HM, Westbrook J, Feng Z, Gilliland G, Bhat TN, Weissig H, Shindyalov IN,
542 Bourne PE. 2000. The Protein Data Bank. Nucleic Acids Res 28:235–242.

543 29. Jumper J, Evans R, Pritzel A, Green T, Figurnov M, Ronneberger O, Tunyasuvunakool
544 K, Bates R, Žídek A, Potapenko A, Bridgland A, Meyer C, Kohl SAA, Ballard AJ,
545 Cowie A, Romera-Paredes B, Nikolov S, Jain R, Adler J, Back T, Petersen S, Reiman
546 D, Clancy E, Zielinski M, Steinegger M, Pacholska M, Berghammer T, Bodenstein S,
547 Silver D, Vinyals O, Senior AW, Kavukcuoglu K, Kohli P, Hassabis D. 2021. Highly
548 accurate protein structure prediction with AlphaFold. Nat 2021 5967873 596:583–589.

549 30. Varadi M, Anyango S, Deshpande M, Nair S, Natassia C, Yordanova G, Yuan D,
550 Stroe O, Wood G, Laydon A, Zídek A, Green T, Tunyasuvunakool K, Petersen S,
551 Jumper J, Clancy E, Green R, Vora A, Lutfi M, Figurnov M, Cowie A, Hobbs N,
552 Kohli P, Kleywegt G, Birney E, Hassabis D, Velankar S. 2022. AlphaFold Protein
553 Structure Database: massively expanding the structural coverage of protein-sequence
554 space with high-accuracy models. Nucleic Acids Res 50:D439–D444.

555 31. Ravala SK, Singh S, Yadav GS, Kumar S, Karthikeyan S, Chakraborti PK. 2015.
556 Evidence that phosphorylation of threonine in the GT motif triggers activation of
557 PknA, a eukaryotic-type serine/threonine kinase from *Mycobacterium tuberculosis.*
558 FEBS J 282:1419–31.

559 32. Pettersen EF, Goddard TD, Huang CC, Couch GS, Greenblatt DM, Meng EC, Ferrin
560 TE. 2004. UCSF Chimera - A visualization system for exploratory research and
561 analysis. J Comput Chem 25:1605–1612.

562 33. R Core Team. 2021. R: A Language and Environment for Statistical Computing. 4.1.0.

563 R Foundation for Statistical Computing, Vienna, Austria.

564 34. Kanda Y. 2013. Investigation of the freely available easy-to-use software "EZR" for
565 medical statistics. Bone Marrow Transplant 48:452–8.

566 35. Ortega C, Liao R, Anderson LN, Rustad T, Ollodart AR, Wright AT, Sherman DR,
567 Grundner C. 2014. *Mycobacterium tuberculosis* Ser/Thr Protein Kinase B Mediates an
568 Oxygen-Dependent Replication Switch. PLOS Biol 12:e1001746.

569 36. Asakura H, Igimi S, Kawamoto K, Yamamoto S, Makino S-I. 2005. Role of in vivo
570 passage on the environmental adaptation of enterohemorrhagic *Escherichia coli*
571 O157:H7: cross-induction of the viable but nonculturable state by osmotic and
572 oxidative stresses. FEMS Microbiol Lett 253:243–9.

573 37. Ducret A, Chabalier M, Dukan S. 2014. Characterization and resuscitation of "non-
574 culturable" cells of *Legionella pneumophila.* BMC Microbiol 14:3.

575 38. Asakura H, Ishiwa A, Arakawa E, Makino S, Okada Y, Yamamoto S, Igimi S. 2007.
576 Gene expression profile of *Vibrio cholerae* in the cold stress-induced viable but non-
577 culturable state. Environ Microbiol 9:869–79.

578 39. Pasquaroli S, Zandri G, Vignaroli C, Vuotto C, Donelli G, Biavasco F. Antibiotic
579 pressure can induce the viable but non-culturable state in *Staphylococcus aureus*
580 growing in biofilms.

581 40. Vilhena C, Kaganovitch E, Grünberger A, Motz M, Forné I, Kohlheyer D, Jung K.
582 2019. Importance of Pyruvate Sensing and Transport for the Resuscitation of Viable
583 but Nonculturable *Escherichia coli* K-12. J Bacteriol 201.

584 41. Wagley S, Morcrette H, Kovacs-Simon A, Yang ZR, Power A, Tennant RK, Love J,
585 Murray N, Titball RW, Butler CS. 2021. Bacterial dormancy: A subpopulation of
586 viable but non-culturable cells demonstrates better fitness for revival. PLoS Pathog
587 17:e1009194.

588 42. Osada-Oka M, Goda N, Saiga H, Yamamoto M, Takeda K, Ozeki Y, Yamaguchi T,

589 Soga T, Tateishi Y, Miura K, Okuzaki D, Kobayashi K, Matsumoto S. 2019.
590 Metabolic adaptation to glycolysis is a basic defense mechanism of macrophages for
591 *Mycobacterium tuberculosis* infection. Int Immunol 31:781–793.
592 43. Schaefer WB. 1952. GROWTH REQUIREMENTS OF DYSGONIC AND EUGONIC
593 STRAINS OF MYCOBACTERIUM TUBERCULOSIS VAR. BOVIS. J Exp Med
594 96:207–219.
595 44. Huang BX, Kim HY, Dass C. 2004. Probing three-dimensional structure of bovine
596 serum albumin by chemical cross-linking and mass spectrometry. J Am Soc Mass
597 Spectrom 15:1237–1247.
598 45. Rombouts I, Lagrain B, Scherf KA, Lambrecht MA, Koehler P, Delcour JA. 2015.
599 Formation and reshuffling of disulfide bonds in bovine serum albumin demonstrated
600 using tandem mass spectrometry with collision-induced and electron-transfer
601 dissociation. Sci Rep 5:12210.
602 46. Broersen K, Van Teeffelen AMM, Vries A, Voragen AGJ, Hamer RJ, De Jongh HHJ.
603 2006. Do sulfhydryl groups affect aggregation and gelation properties of ovalbumin? J
604 Agric Food Chem 54:5166–74.
605 47. Hamabata T, Senoh M, Iwaki M, Nishiyama A, Yamamoto A, Shibayama K. 2021.
606 Induction and Resuscitation of Viable but Nonculturable *Corynebacterium*
607 *diphtheriae*. Microorganisms 9.
608 48. Liu J, Li L, Peters BM, Li B, Chen L, Deng Y, Xu Z, Shirtliff ME. 2017. The viable
609 but nonculturable state induction and genomic analyses of *Lactobacillus casei* BM-
610 LC14617, a beer-spoilage bacterium. Microbiologyopen 6.
611 49. Morishige Y, Koike A, Tamura-Ueyama A, Amano F. 2017. Induction of viable but
612 nonculturable *Salmonella* in exponentially grown cells by exposure to a low-humidity
613 environment and their resuscitation by catalase. J Food Prot 80:288–294.
614 50. Kong HG, Bae JY, Lee HJ, Joo HJ, Jung EJ, Chung E, Lee S-W. 2014. Induction of

615 the viable but nonculturable state of *Ralstonia solanacearum* by low temperature in the
616 soil microcosm and its resuscitation by catalase. PLoS One 9:e109792.
617 51. Kong I-S, Bates TC, HÃ¼lsmann A, Hassan H, Smith BE, Oliver JD. 2004. Role of
618 catalase and oxyR in the viable but nonculturable state of *Vibrio vulnificus*. FEMS
619 Microbiol Ecol 50:133–142.
620 52. Senoh M, Hamabata T, Takeda Y. 2015. A factor converting viable but nonculturable
621 *Vibrio cholerae* to a culturable state in eukaryotic cells is a human catalase.
622 Microbiologyopen 4:589–96.
623 53. Manuse S, Fleurie A, Zucchini L, Lesterlin C, Grangeasse C. 2016. Role of
624 eukaryotic-like serine/threonine kinases in bacterial cell division and morphogenesis.
625 FEMS Microbiol Rev 40:41–56.
626 54. Carette X, Platig J, Young DC, Helmel M, Young AT, Wang Z, Potluri L-P, Moody
627 CS, Zeng J, Prisic S, Paulson JN, Muntel J, Madduri AVR, Velarde J, Mayfield JA,
628 Locher C, Wang T, Quackenbush J, Rhee KY, Moody DB, Steen H, Husson RN. 2018.
629 Multisystem Analysis of *Mycobacterium tuberculosis* Reveals Kinase-Dependent
630 Remodeling of the Pathogen-Environment Interface. MBio 9.
631 55. Thakur M, Chakraborti PK. 2008. Ability of PknA, a mycobacterial eukaryotic-type
632 serine/threonine kinase, to transphosphorylate MurD, a ligase involved in the process
633 of peptidoglycan biosynthesis. Biochem J 415:27–33.
634 56. Parikh A, Verma SK, Khan S, Prakash B, Nandicoori VK. 2009. PknB-mediated
635 phosphorylation of a novel substrate, N-acetylglucosamine-1-phosphate
636 uridyltransferase, modulates its acetyltransferase activity. J Mol Biol 386:451–64.
637 57. Jagtap PKA, Soni V, Vithani N, Jhingan GD, Bais VS, Nandicoori VK, Prakash B.
638 2012. Substrate-bound crystal structures reveal features unique to *Mycobacterium*
639 *tuberculosis* N-acetyl-glucosamine 1-phosphate uridyltransferase and a catalytic
640 mechanism for acetyl transfer. J Biol Chem 287:39524–37.

641 58. Gee CL, Papavinasasundaram KG, Blair SR, Baer CE, Falick AM, King DS, Griffin
642 JE, Venghatakrishnan H, Zukauskas A, Wei J-R, Dhiman RK, Crick DC, Rubin EJ,
643 Sassetti CM, Alber T. 2012. A phosphorylated pseudokinase complex controls cell
644 wall synthesis in mycobacteria. Sci Signal 5:ra7.
645 59. Kang C-M, Nyayapathy S, Lee J-Y, Suh J-W, Husson RN. 2008. Wag31, a homologue
646 of the cell division protein DivIVA, regulates growth, morphology and polar cell wall
647 synthesis in mycobacteria. Microbiology 154:725–735.
648 60. Gupta M, Sajid A, Sharma K, Ghosh S, Arora G, Singh R, Nagaraja V, Tandon V,
649 Singh Y. 2014. HupB, a nucleoid-associated protein of *Mycobacterium tuberculosis*, is
650 modified by serine/threonine protein kinases *in vivo*. J Bacteriol 196:2646–57.
651 61. Baronian G, Ginda K, Berry L, Cohen-Gonsaud M, Zakrzewska-Czerwińska J,
652 Jakimowicz D, Molle V. 2015. Phosphorylation of *Mycobacterium tuberculosis* ParB
653 participates in regulating the ParABS chromosome segregation system. PLoS One
654 10:e0119907.
655 62. Thakur M, Chakraborti PK. 2006. GTPase activity of mycobacterial FtsZ is impaired
656 due to its transphosphorylation by the eukaryotic-type Ser/Thr kinase, PknA. J Biol
657 Chem 281:40107–13.
658 63. Sureka K, Hossain T, Mukherjee P, Chatterjee P, Datta P, Kundu M, Basu J. 2010.
659 Novel role of phosphorylation-dependent interaction between FtsZ and FipA in
660 mycobacterial cell division. PLoS One 5:e8590.
661 64. Wright DP, Ulijasz AT. 2014. Regulation of transcription by eukaryotic-like serine-
662 threonine kinases and phosphatases in gram-positive bacterial pathogens. Virulence
663 5:863–885.
664 65. Rock JM, Hopkins FF, Chavez A, Diallo M, Chase MR, Gerrick ER, Pritchard JR,
665 Church GM, Rubin EJ, Sassetti CM, Schnappinger D, Fortune SM. 2017.
666 Programmable transcriptional repression in mycobacteria using an orthogonal CRISPR

667 interference platform. Nat Microbiol 2:16274.

668 66. Minato Y, Gohl DM, Thiede JM, Chacón JM, Harcombe WR, Maruyama F, Baughn
669 AD. 2019. Genomewide Assessment of *Mycobacterium tuberculosis* Conditionally
670 Essential Metabolic Pathways. mSystems 4.

671 67. DeJesus MA, Gerrick ER, Xu W, Park SW, Long JE, Boutte CC, Rubin EJ,
672 Schnappinger D, Ehrt S, Fortune SM, Sassetti CM, Ioerger TR. 2017. Comprehensive
673 Essentiality Analysis of the *Mycobacterium tuberculosis* Genome via Saturating
674 Transposon Mutagenesis. MBio 8.

675 68. Sassetti CM, Boyd DH, Rubin EJ. 2003. Genes required for mycobacterial growth
676 defined by high density mutagenesis. Mol Microbiol 48:77–84.

677 69. Griffin JE, Gawronski JD, Dejesus MA, Ioerger TR, Akerley BJ, Sassetti CM. 2011.
678 High-resolution phenotypic profiling defines genes essential for mycobacterial growth
679 and cholesterol catabolism. PLoS Pathog 7:e1002251.

680

681

682

683

684

685

686

687

688

689 **Figure legends**

690 Figure 1. Growth curves of Mtb H37Rv cells in Dubos medium in the presence or absence of
691 BSA

692 (A) Number of culturable cells in Dubos medium in the presence (closed circle) or
693 absence (open circle) of 0.1% BSA at the indicated days of incubation. The CFU/mL
694 values were determined by plating cells onto 7H10 plates in duplicate. Data represent
695 the mean ± SD from three independent experiments.
696 (B) Representative images of Mtb growth captured at the end of incubation.

697 Figure 2. Viability analyses of DPI-treated Mtb

698 (A) Number of culturable cells after DPI treatment. The CFU/mL values were determined
699 by plating cells onto 7H10 plates in duplicate. Asterisk indicates a statistically
700 significant difference (*$p < 0.05$, Welch's *t*-test). Data represent the mean ± SD from
701 three independent experiments.
702 (B) Percentages of esterase active cells after DPI treatment. Around 850 cells were
703 directly counted under 100× objective lens. Data represent the mean ± SD from three
704 independent experiments.
705 (C) Merged fluorescence micrographs of Mtb H37Rv cells stained with
706 carboxyfluorescein diacetate (CFDA) and ethidium bromide (EtBr). Cells stained with
707 CFDA (green) are esterase-positive; those stained with EtBr (red) are membrane-
708 damaged. Images are representative images from three individual experiments. Scale
709 bar: 2μm
710 (D) Percentage of acid-fast-positive cells (open column) or acid-fast-negative but lipid-
711 accumulation-positive cells (gray column). Approximately 1,100 cells were directly
712 counted under 100× objective lens. Data represent the mean ± SD from four

713 independent experiments. Asterisk indicates significant difference (***$p < 0.005$,
714 Welch's *t*-test).
715 (E) Merged fluorescence micrographs of Mtb H37Rv cells stained with auramine-O and
716 Nile Red. Cells stained with auramine-O (green) are acid-fast-positive; those stained
717 with Nile Red (red) are acid-fast-negative but lipid accumulation-positive. Images are
718 representative images from three individual experiments. Scale bar: 2μm
719 (F) Magnified views of Airyscan confocal super-resolution microscopy observation of
720 three different Mtb cells obtained from DPI-treated culture. Only acid-fast-positive
721 cells (left), both acid-fast-positive and lipid accumulation-positive cells (center,
722 counted as acid-fast-positive) and acid-fast-negative cells with only lipid
723 accumulation-positive cells (right). Dual-positive cells probably represent the
724 transition to a non-culturable state. Indicated foci with arrowheads represent a neutral
725 lipid body. Scale bar: 1 μm

726 Figure 3. Reactivation of DPI-treated Mtb H37Rv cells by FBS and OADC supplementation

727 (A) Number of culturable cells at the indicated days of incubation, without
728 supplementation or those cells supplemented with 2% FBS or 10% OADC in the
729 presence (closed circle) or absence (open circle) of 0.1% BSA. The CFU/mL values
730 were determined by plating cells onto 7H10 plates in duplicate. Data represent the
731 mean ± SD from three independent experiments. U.D. means under the limit of
732 detection (20 CFU/mL).
733 (B) Representative images of regrowth under the indicated conditions captured at the end
734 of incubation. None, FBS, and OADC represent no supplementation, 2% FBS and
735 10% OADC supplementation, respectively.

736 Figure 4. Effect of human serum albumin, ovalbumin and antioxidants on the reactivation of

737 DPI-treated Mtb.

738 (A) Number of culturable cells at the end of incubation, supplemented with albumins or
739 antioxidative agents. The CFU/mL values were determined by plating cells onto 7H10
740 plates in duplicate. Data represent the mean ± SD from three independent
741 experiments. Asterisk indicates a statistically significant difference between Day 0
742 and Day 20 by Student's *t*-test. (*$p<0.05$)
743 (B) Representative images of regrowth captured at the end of incubation.

744 Abbreviations:
745 BSA, bovine serum albumin; HSA, human serum albumin; OVA, ovalbumin; NAC, N-
746 acetyl-L-cysteine; MAN, D-mannitol.
747 The final concentrations of each reagent were as follows:
748 BSA, HSA and OVA: 0.1% (w/v), NAC: 500 μM, MAN: 50 mM.

749 Figure 5. The effect of SQ22536 or H89 or staurosporine on the reactivation of DPI-treated
750 Mtb

751 (A) Number of culturable cells at the end of incubation, supplemented with 0.1% BSA
752 and SQ22536 or H89 or staurosporine. Inhibitor was added at the indicated
753 concentration.
754 (B) Representative images of regrowth captured at the end of incubation.

755 The CFU/mL values were determined by plating cells onto 7H10 plates in duplicate. Data
756 represent the mean ± SD from three independent experiments.

757 Figure 6. Schematic representation of the mechanism of BSA-induced reactivation of Mtb.
758 Although the detailed mechanism of interaction between BSA and PknA/PknB is not yet

759 clear, BSA may activate PknA/PknB and positively regulate target proteins that are involved
760 in the localized synthesis of peptidoglycan, cell division control, and DNA condensation and
761 partitioning through their phosphorylation, resulting in the reactivation of VBNC Mtb cells.

(A)

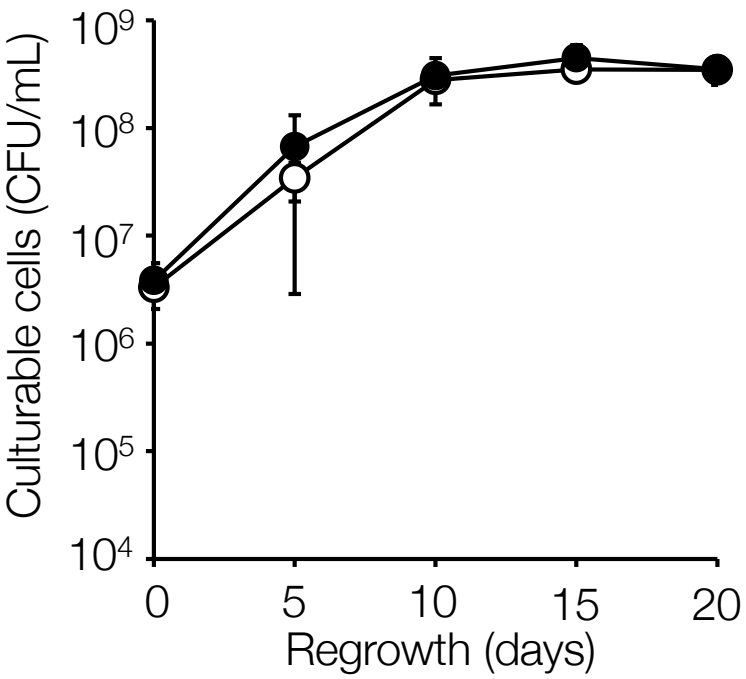
Culturable cells (CFU/mL)
10^9
10^8
10^7
10^6
10^5
10^4
0
5
10
15
20
Regrowth (days)

(B)

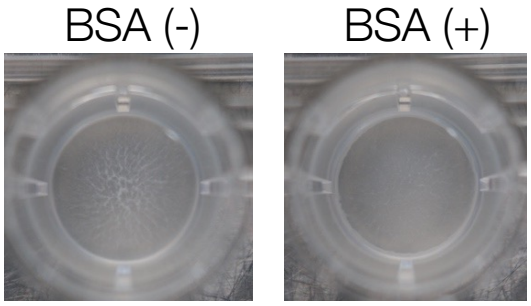
BSA (-)
BSA (+)

Fig 1.

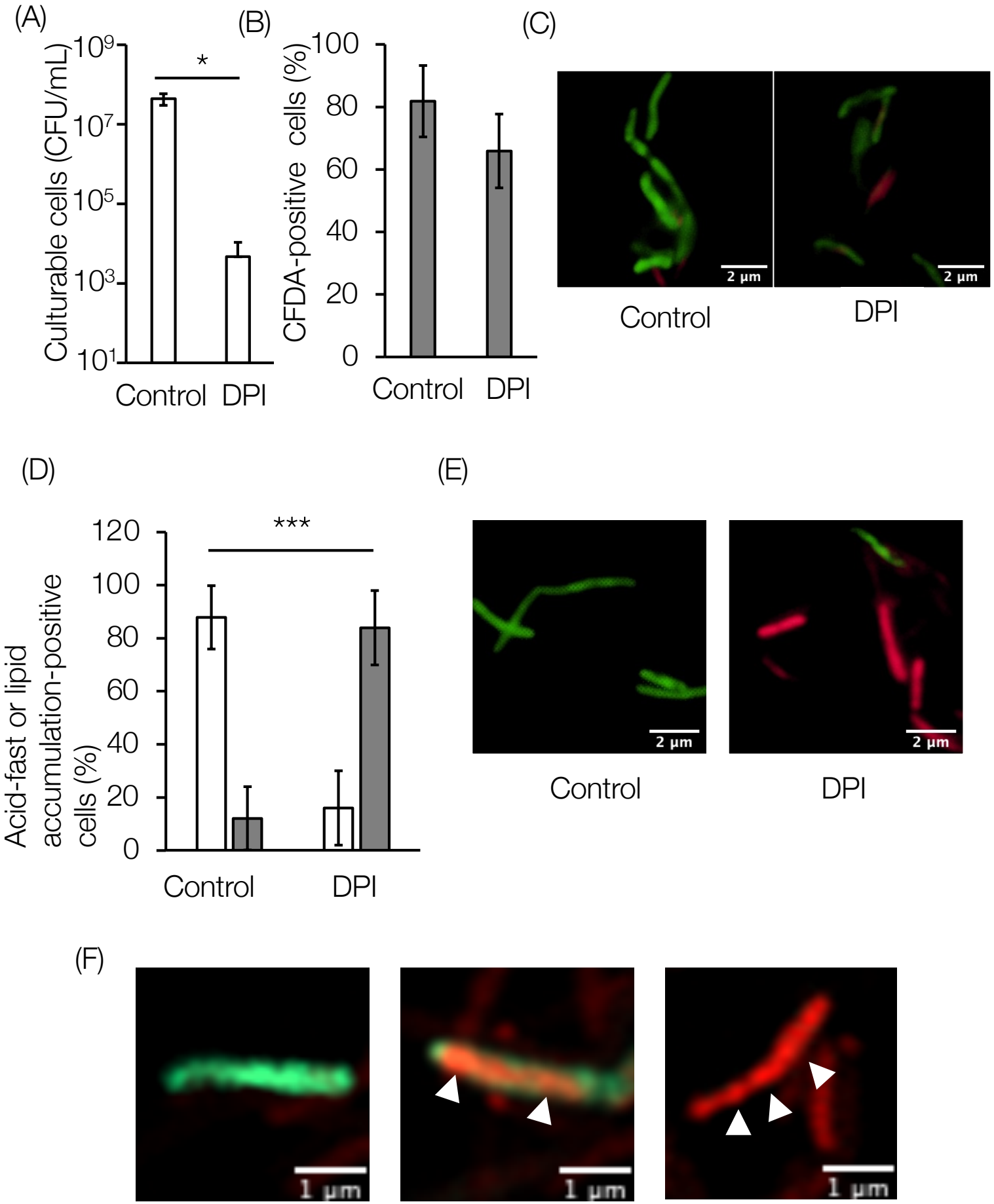
(A)
Culturable cells (CFU/mL)
10^9
10^7
10^5
10^3
10^1
*
Control
DPI
(B)
CFDA-positive cells (%)
100
80
60
40
20
0
Control
DPI
(C)
2 μm
2 μm
Control
DPI
(D)
Acid-fast or lipid accumulation-positive cells (%)
120
100
80
60
40
20
0
***
Control
DPI
(E)
2 μm
2 μm
Control
DPI
(F)
1 μm
1 μm
1 μm

Fig 2.

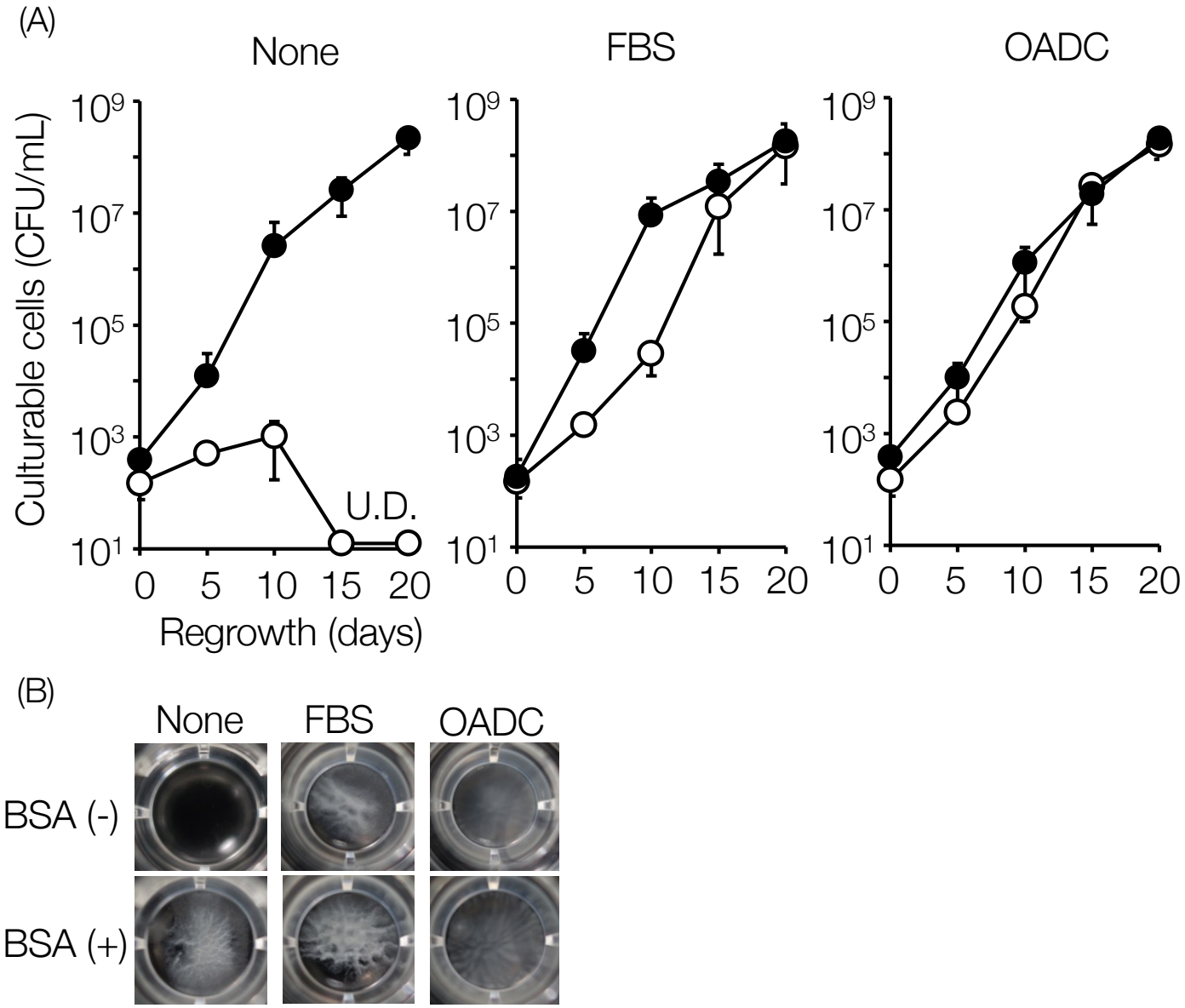
(A)
None
FBS
OADC
Culturable cells (CFU/mL)
10^9
10^7
10^5
10^3
10^1
U.D.
0 5 10 15 20
Regrowth (days)
(B)
None
FBS
OADC
BSA (-)
BSA (+)

Fig 3.

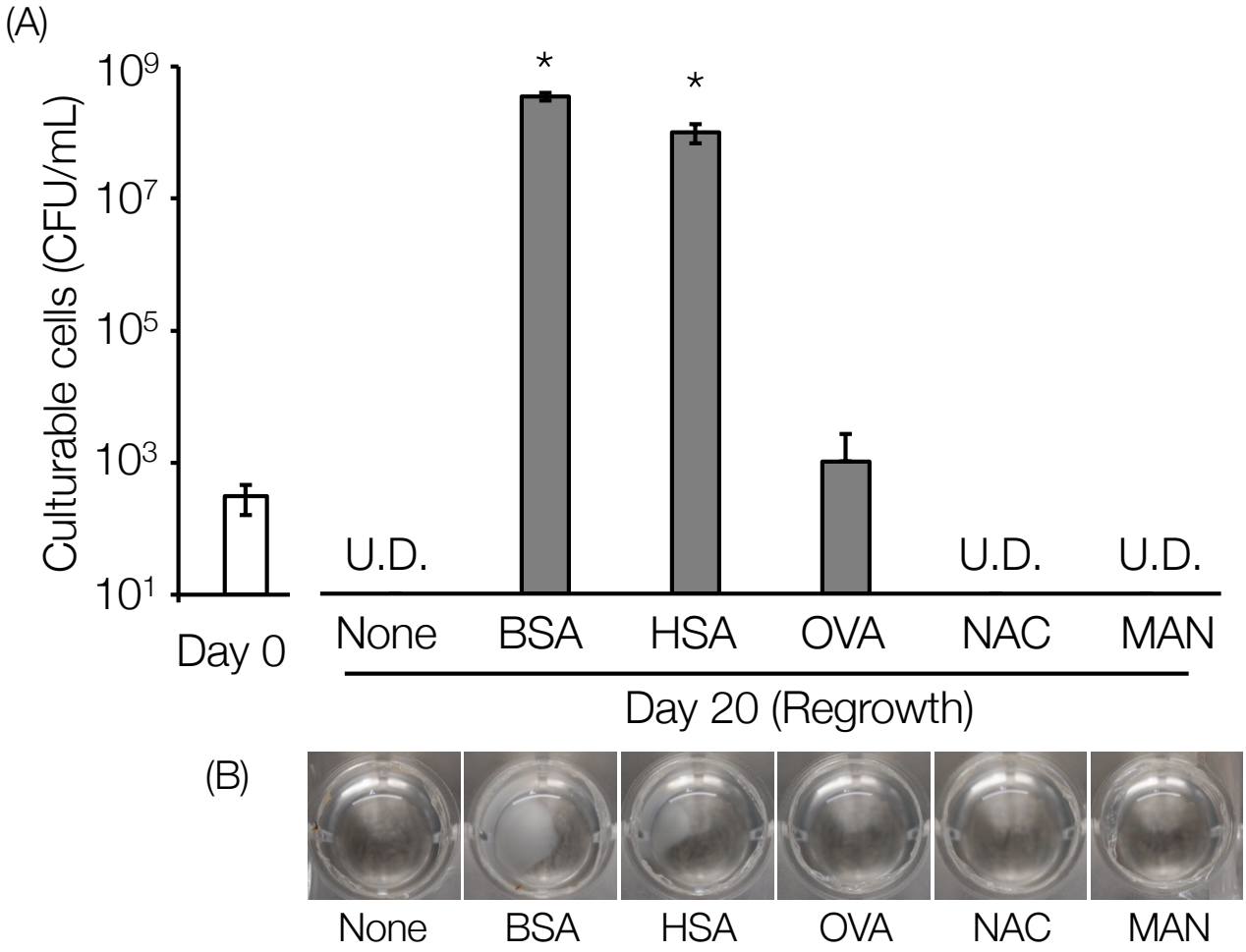
(A)
Culturable cells (CFU/mL)
10^9
10^7
10^5
10^3
10^1
*
*
U.D.
U.D.
U.D.
Day 0
None
BSA
HSA
OVA
NAC
MAN
Day 20 (Regrowth)
(B)
None
BSA
HSA
OVA
NAC
MAN

Fig 4.

(A)

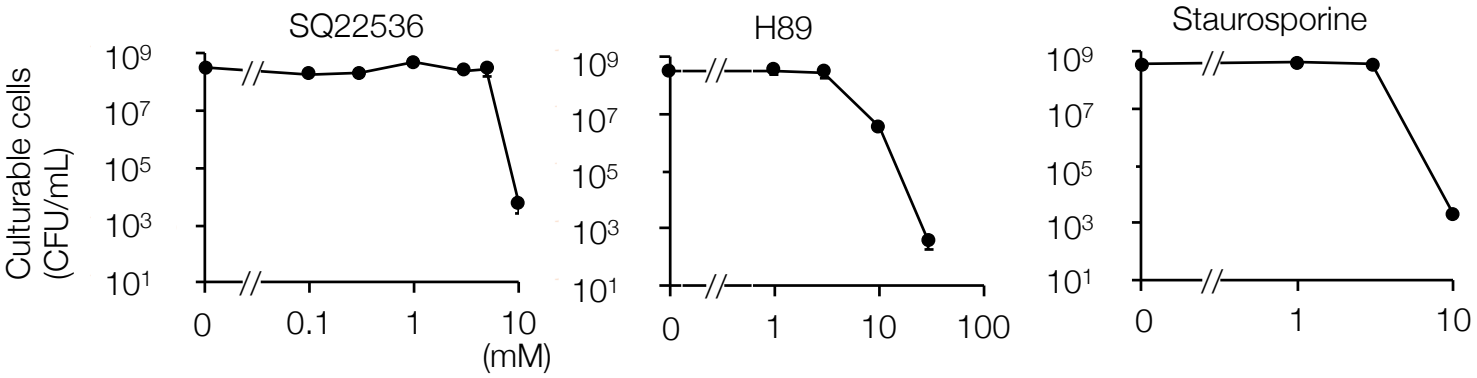
SQ22536
H89
Staurosporine
Culturable cells (CFU/mL)
10^9
10^7
10^5
10^3
10^1
0
0.1
1
10
100
(mM)

(B)

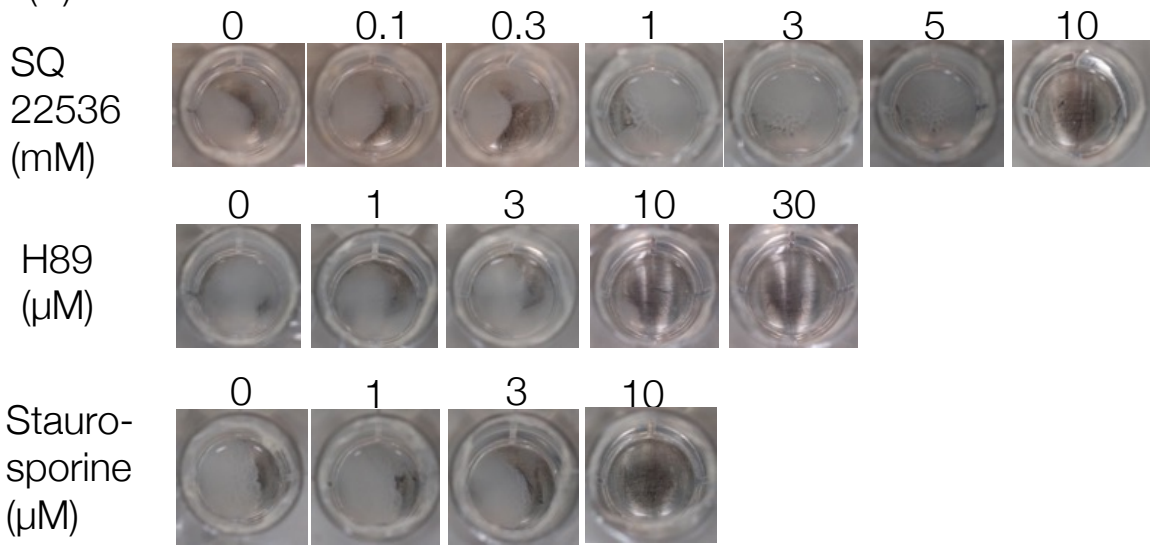
SQ 22536 (mM)
0
0.1
0.3
1
3
5
10
H89 (μM)
0
1
3
10
30
Stauro-sporine (μM)
0
1
3
10

Fig 5.

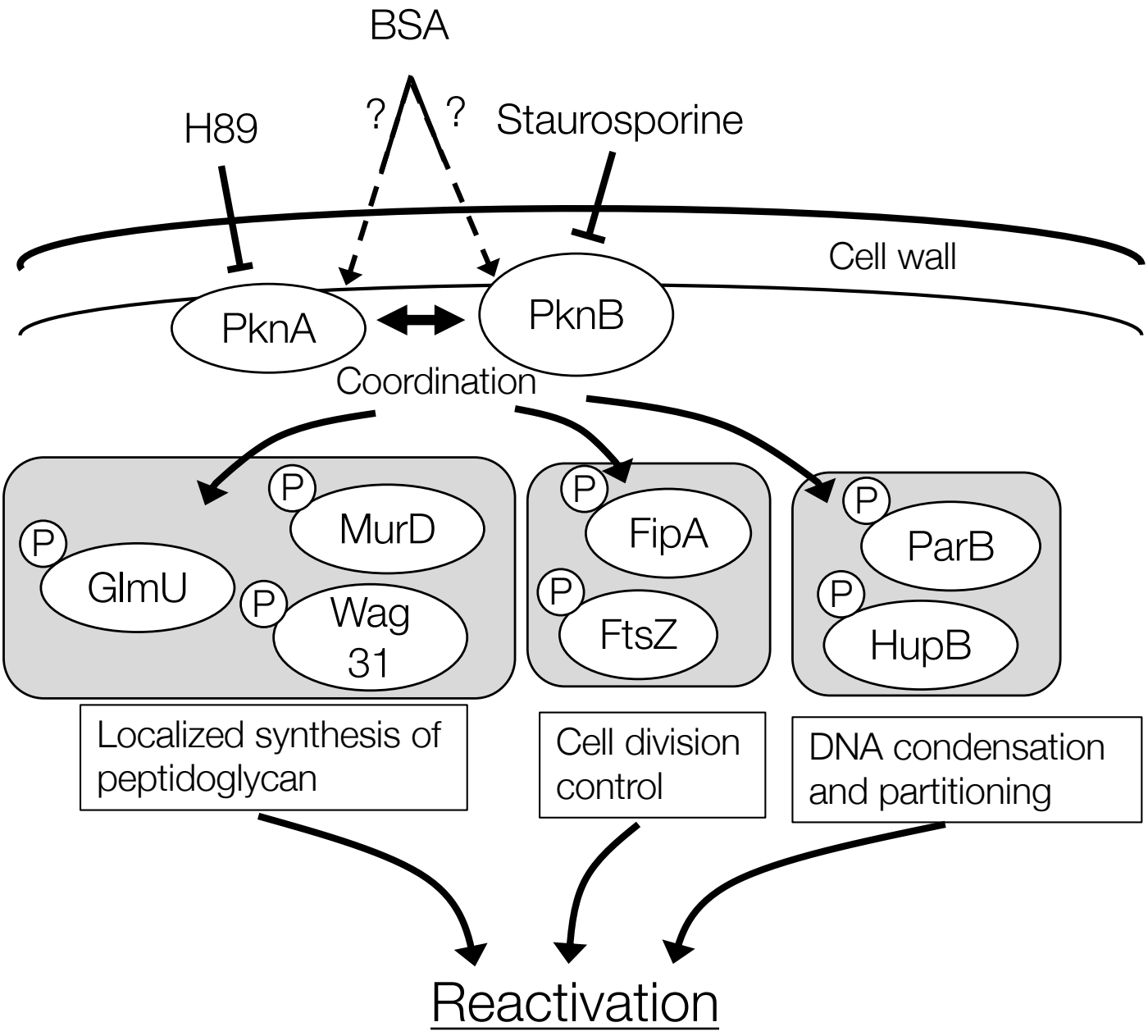
BSA
H89
?
?
Staurosporine
Cell wall
PknA
PknB
Coordination
P
MurD
P
GlmU
P
Wag
31
P
FipA
P
FtsZ
P
ParB
P
HupB
Localized synthesis of peptidoglycan
Cell division control
DNA condensation and partitioning
Reactivation

Fig. 6